Available online at www.sciencedirect.com

SCIENCE DIRECT

Brain Research 1016 (2004) 182–194

BRAIN RESEARCH

www.elsevier.com/locate/brainres

Research report

Two types of afferent terminals innervate cochlear inner hair cells in C57BL/6J mice

Howard W. Francis[a,*], Alejandro Rivas[a], Mohamed Lehar[a], David K. Ryugo[a,b]

[a] *Department of Otolaryngology-Head and Neck Surgery, Johns Hopkins University, 720 Rutland Avenue, Baltimore, MD 21205, USA*
[b] *Department of Neuroscience, Johns Hopkins University, 720 Rutland Avenue, Baltimore, MD 21205, USA*

Accepted 1 May 2004
Available online 19 June 2004

Abstract

Afferent synapses on inner hair cells (IHC) transfer auditory information to the central nervous system (CNS). Despite the importance of these synapses for normal hearing, their response to cochlear disease and dysfunction is not well understood. The C57BL/6J mouse is a model for presbycusis and noise-induced hearing loss because of its age-related hearing loss and susceptibility to acoustic over-exposure. In this context, we sought to establish normal synaptic structure in order to better evaluate synaptic changes due to presbycusis and noise exposure. Ultrastructural analysis of IHCs and afferent terminals was performed in a normal hearing 3-month-old C57BL/6J mouse at cochlear sites corresponding to 8, 16 and 32 kHz using semi-serial sections. A stereologic survey of random sections was conducted of IHCs in 11 additional mice. Two morphologically distinct groups of afferent terminals were identified at all 3 frequency locations in 11 out of 12 animals. ''Simple'' endings demonstrated classic features of bouton terminals, whereas ''folded'' endings were larger in size and exhibited a novel morphologic feature that consisted of a fully internalized double membrane that partially divided the terminal into two compartments. In many cases, the double membrane was continuous with the outer terminal membrane as if produced by an invagination. We still must determine the generality of these observations with respect to other mouse strains.

Theme: Sensory systems
Topic: Auditory, vestibular and lateral line: periphery

Keywords: Inner hair cell; Auditory; Synapse; Nerve ending; Mitochondria; Presbycusis

1. Introduction

Auditory nerve terminals and their synaptic relationships with inner hair cells (IHC) represent physiologically important links between the mechano-electric transduction of sound in the organ of Corti and the delivery of acoustic information to the central nervous system (CNS). The frequency content and intensity of sounds are encoded with great fidelity by individual auditory nerve fibers whose discharge properties determine their role in signal processing [15,18,34,47]. Knowledge about the biological substrates that underlie these functional characteristics is a prerequisite for understanding disorders of this system and for planning therapeutic strategies.

Structural correlates of afferent transduction, particularly the pre- and post-synaptic components, may yield useful insights into biological mechanisms of hearing. Spontaneous firing rate and other discharge characteristics that determine the encoding properties of individual nerve fibers are likely to depend on synaptic function [16,44] and are related to synaptic and terminal morphometry [19,20,23]. Reduction in cortical synaptic density and increase in synaptic size, for example, are associated with cognitive decline in humans [1] and senescence in laboratory animals [2]. Similar changes in the synaptic relationship between afferent dendrites and IHCs may account for hearing impairment, particularly speech discrimination deficits in noise, but are beyond the resolving power of the light

* Corresponding author. 601 N. Caroline Street, JHOC 6251, Baltimore, MD 21287-0910, USA. Tel.: +1-410-955-1640; fax: +1-410-614-8610.
E-mail address: hfrancis@jhmi.edu (H.W. Francis).

0006-8993/$ - see front matter © 2004 Elsevier B.V. All rights reserved.
doi:10.1016/j.brainres.2004.05.016

microscope [8,36]. Pathology at afferent terminals and their synapses might explain changes in the distribution of low- and high-spontaneous rate fibers in cats with noise-induced hearing loss [21] or in gerbils with age-induced hearing loss [35]. Although denervation of an IHC by intact afferent terminals has been demonstrated in a single human temporal bone with Meniere's disease [28], the study of synaptic structure in humans is generally jeopardized by postmortem decomposition occurring prior to tissue fixation.

The C57BL/6J mouse strain has proven to be a particularly useful animal model for the study of noise-induced [17,30] and age-related hearing impairment [13,14] because of its heightened vulnerability. As in humans with presbycusis this strain experiences a deterioration of frequency resolution reflected by poor hearing in noise [31] that precedes notable light microscopic changes in the organ of Corti [9]. The afferent innervation of IHCs has not been well characterized in the C57BL/6J mouse, so we conducted a transmission electron microscopic (TEM) study to describe the normal structure. These data will be useful for future comparison to functionally impaired ears or the ears of transgenic mice with a C57BL/6J genetic background in which relevant genes have been manipulated.

2. Materials and methods

Cochlear tissue was collected from C57BL/6J mice in accordance with procedures approved by the Animal Care and Use Committee of Johns Hopkins University. A semi-serial section analysis of IHC innervation was conducted using transmission electron microscopy (TEM) at 8, 16 and 32 kHz sites in the left cochlea of a 3-month-old mouse, C57-29, that demonstrated normal auditory brainstem response thresholds at these frequencies. A survey of IHCs in random sections taken from 11 other C57BL/6J mice was also conducted that confirmed the generality of observations made in the first animal (Table 1).

Table 1
C57BL/6J mice studied

Animal (ear)	Age (months)	Cochlear region(s)	No. IHCs examined	Ave. section interval	Folded terminals
C57-29L	3	8, 16, 32 kHz	4, 3, 3	2.2, 1.0, 1.0	observed
C57-28L	3	21 kHz	3	3.7	not observed
C57-35R	2	8, 16 kHz	3, 4	7.6	observed
C57-36L	2	16 kHz	4	6.7	observed
C57-47L	5	mid-base	3	8.1	observed
C57-55L	2	21 kHz	3	2.5	observed
C57-53L	2	16 kHz	3	16.1	observed
C57-54L	2	16 kHz	3	2.8	observed
C57-56L	2	16 kHz	3	2.5	observed
C57-59L	2	16 kHz	3	7.3	observed
C57-MilesR	8	16 kHz	2	4.1	observed
C57-JanisL	8	16 kHz	3	1.0	observed

In order to minimize tissue artifacts due to hypoxia and other post-mortem effects, each cochlea was perfused with fixative while the animal was spontaneously breathing under general anesthesia. Following the intraperitoneal administration (5 ml/kg, i.p.) of a mixture of ketamine (25 mg/ml), xylazine (2.5 mg/ml) and ethanol (14.25%), the animal was placed in a fume hood where its head was stabilized using a bite bar. The middle ear was entered through a post-auricular incision and visualized using an operating microscope. No outer or middle ear pathology was encountered in any of the animals studied. The stapedial artery was exposed as it crossed the oval window by removing the posterior edge of the tympanic bone. The artery was cauterized using fine-tipped bipolar forceps (Assi PowerMate, Accurate Surgical), and the cochlear apex was gently fenestrated with a pick producing free flow of perilymph. The stapes and its footplate were removed from the oval window through which 1% OsO_4/1% potassium ferricyanide (KFeCN) was perfused using a Pasteur pipette with a tightly fitting flamed tip. Tissue fixation was achieved by perfusing the cochlea continuously with a syringe pump at a rate of 3–5 cm^3/min for 5 min while the animal was alive, followed by decapitation, opening of the round window, and resumption of cochlear perfusion through both oval and round windows within 3 min for an additional 10 min. The appearance of a dark stripe representing the cochlear lateral wall indicated a successful perfusion. Care was taken to observe the animal's respirations throughout the procedure until decapitation. If labored breathing or apnea were observed during perfusion, the animal was immediately decapitated, the bulla widely opened and perfusion resumed within 3 min. The heads were then submerged in 1% OsO_4/1% KFeCN for an additional 45 min prior to the removal of the temporal bones. Because optimal fixation of afferent terminals was usually achieved in the first ear to be perfused (left ear), no attempt was made to prepare the contralateral ear for electron microscopy.

The cochleae were removed using fine rongeurs, decalcified with 0.1 M EDTA (with 1% glutaraldehyde), dehydrated in graded alcohols and propylene oxide, and then embedded in Araldite [9,14]. The cochleae were sectioned parallel to the modiolus at 40-μm thickness and mounted between sheets of Aclar for light microscopic analysis (Fig. 1A). Each section was traced using a drawing tube and the junction of the inner and outer pillar cells was labeled. Tracings were digitized, and using either NIH image and Voxblast (Vaytech) or Neuroleucida (Microbrightfield), were stacked in series creating a three-dimensional spiral along the organ of Corti (Fig. 1B). A mouse frequency-place map [4] was used to identify the 8-, 16- and 32-kHz cochlear sites for subsequent examination with transmission electron microscopy. A cochlear frequency-map for the CBA/J mouse with a steeper length to frequency slope has been recently derived from recordings in the cochlear nucleus and retrograde tracings of auditory nerve fibers

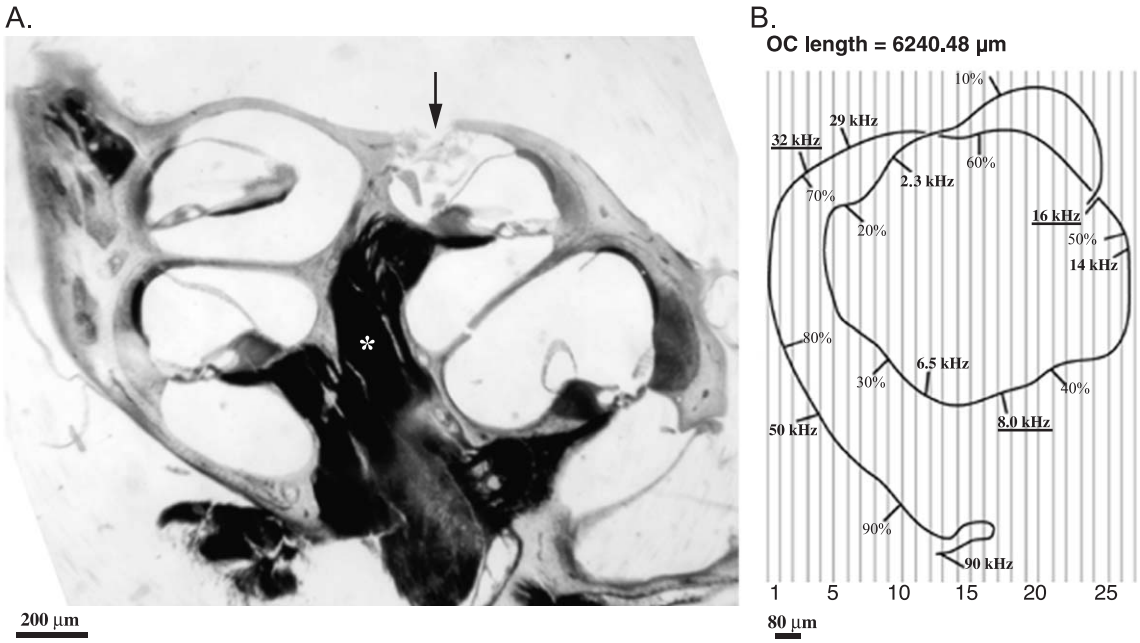

Fig. 1. Method of cochlear reconstruction. (A) Forty-micrometer-thick cochlear sections such as this mid-modiolar section were traced, imported into image-processing software (see methods) and aligned. The modiolus (asterisk) is the core of the cochlea that contains the central axons of spiral ganglion cells. Note the apical fenestration (arrow) made to facilitate intracochlear perfusion of reagents. (B) Apical view of three-dimensional reconstruction of the basilar membrane (see Section 2). Frequency location was assigned using a cochlear frequency map estimated for mouse by Ehret [4] based on percent distance from the apex. OC, organ of Corti.

[25]. The cochlear regions selected for study may therefore correspond to higher frequencies than were actually intended (14, 23 and 37 kHz; M. Mueller, personal communication).

Four cochleae were prepared as whole mounts as described by Liberman in the cat [19], so as to minimize any negative effects of decalcification on afferent ultrastructure. Following dehydration with graded alcohols and propylene oxide, the cochleae were infiltrated with increasing concentrations of Epon, and then polymerized for 3 days in an oven at 60 °C. The surrounding Epon and otic capsule were ground away under the dissection microscope using a drill, after which the cochlea was sectioned into two halves through the modiolus using razor blades and the basilar membrane dissected into half turns. Segments of basilar membrane measuring up to 1 mm were then flat-embedded in Epon. These pieces were arranged in order from the apex, examined under the light microscope, traced with a drawing tube and measured. The pieces containing the frequency regions of interest were selected using the Ehret mouse cochlear-frequency map, sectioned in a radial orientation at 50 μm thickness and mounted between Aclar sheets.

The organ of Corti was excised from the section of interest, embedded in a BEEM capsule, and cut approximately perpendicular to the long axis of the IHC at a setting of 75 nm (Fig. 2A). Ultrathin sections were placed in series on Formvar grids and stained with uranyl acetate. In the case of mouse C57-29L, transmission electron micrographs of every second to fourth section were taken of IHCs in the 8-, 16- and 32-kHz regions starting at the cuticular plate or just above the nucleus and ending several sections below the inferior pole of the cell. Electron micrographs were taken using a Jeol JEM-100CX II microscope at 60 kV and at a magnification of 2700 (Fig. 2B). The average section interval between photographs was 2.2 (S.D. 1.7) in the 8-kHz region, 1.0 (S.D. 0.6) in the 16-kHz region and 1.0 (S.D. 0.3) in the 32-kHz region. A less detailed and random survey of cross sections was performed in the remaining 11 mice (Table 1). Electron micrograph negatives were digitized at a fixed resolution of 400 dpi using the Agfa P2000XL or Leafscan 45 scanners. The resulting images were aligned with a PC application called serial EM (sEM) available online at www.synapses.mcg.edu/lab/howto/mito.htm, using the absolute mode [7]. Inner hair cells and nerve endings in the C57-29L mouse cochlea were traced and stacked in series using imaging software (Neurolucida, Microbrightfield, Essex, VT) (Fig. 2C). Average section thickness was determined separately for each block of tissue using the minimal folds method [3,6]. Folds were randomly photographed in every 10th section. Following digitization and scale calibration in Neuroleucida, fold width was measured at its narrowest point in triplicate and divided by 2 to estimate section thickness. Average fold thicknesses of 78.7 nm (S.D. 13.8 nm), 87.8 nm (S.D. 17.9 nm) and 79.3 nm (S.D. 20.6 nm) were measured for sections from tissue blocks corresponding to 8-, 16- and 32-kHz regions, respectively. The number, size and morphologic features of nerve endings and their synapses were noted for four IHCs at 8 kHz, three at 16 kHz and three at 32 kHz. Terminal apposition area, synaptic area, terminal volume

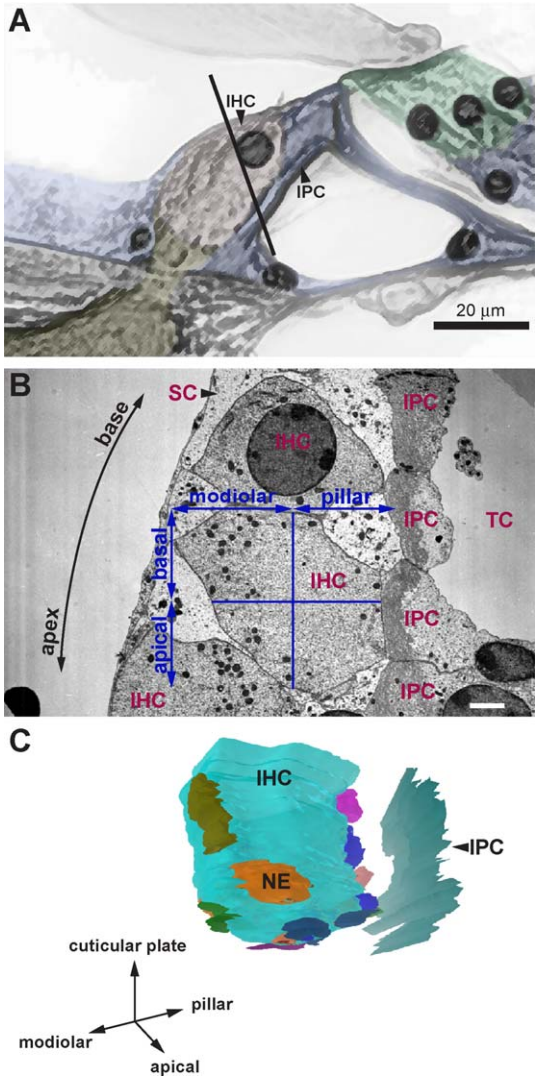

Fig. 2. Method of analysis of transmission electron micrographs. (A) Schematic of organ of Corti showing the orientation of ultrathin sectioning through IHCs. The line indicates the plane of section that is approximately perpendicular to the long axis of the cell. (B) Transmission electron micrograph of resulting cross section through three adjacent IHCs (2700 magnification). The spatial location of terminal boutons innervating each IHC is defined by the coordinate system shown. The row of pillar cells serves as the reference axis that is intersected at right angles in the center of the cell to form pillar, modiolar, apical and basal sectors around the IHC (Scale bar = 2 μm). (C) View of reconstructed infra-nuclear portion of the IHC (blue) and innervating nerve terminals (various colors) facing towards the cochlear apex. Abbreviations: IPC, inner pillar cell; SC, supporting cell; NE, nerve ending; TC, tunnel of Corti.

and other measurements were derived from three-dimensional reconstructions (Fig. 2C) using NeuroExplorer software (Microbrightfield, Essex, VT).

3. Results

Most neuronal processes terminated below the IHC nucleus where they formed afferent synaptic membrane specializations. As previously defined in mouse [40,41], guinea pig [11], cat [19] and human [26], the ultrastructural features associated with the afferent synapse included a well-circumscribed electron-dense plaque formed by the asymmetric thickening of apposing membranes (Fig. 3), which sometimes obliterated the intervening synaptic cleft. As described in other species [11,26,27], most but not all of these synapses had an electron-dense synaptic body (SB)

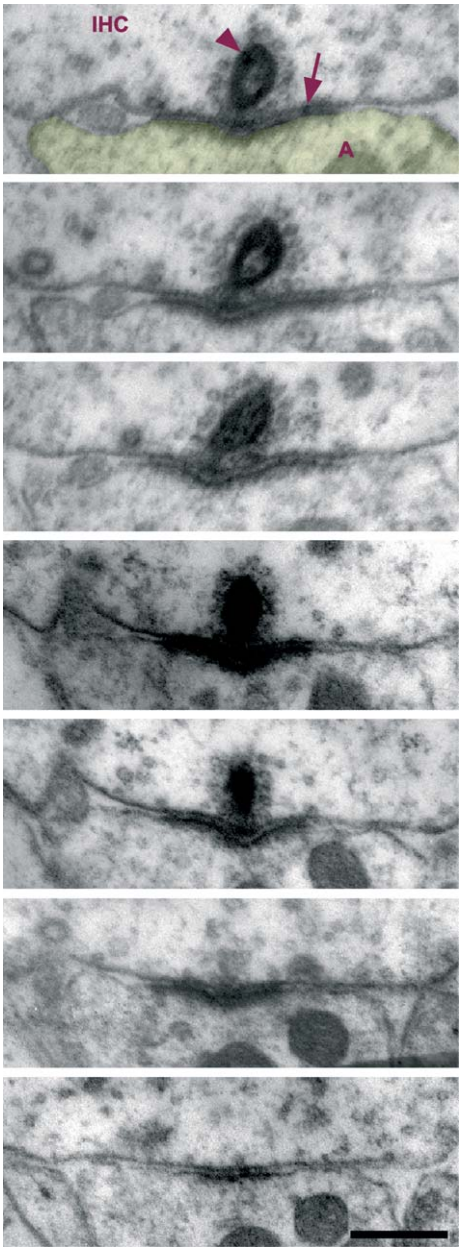

Fig. 3. Serial EM sections through afferent synapse between IHC and afferent terminal (A). This afferent synapse demonstrates asymmetric electron dense thickening of apposing pre- and post-synaptic membranes (arrow), and an electron dense synaptic body (arrowhead), surrounded by a halo of vesicles that appears to be centered over the membrane thickenings. Afferent nerve terminals were identified by the presence of this asymmetric membrane thickening at their contacts with IHCs, with or without a synaptic body. Scale bar = 0.25 μm.

within the IHC (Fig. 3), which was usually surrounded by a halo of clear vesicles. A SB was present in 84% (146/174) of terminals in mouse C57-29: 73% of afferent synapses had a single SB, 11% had 2. Afferent terminals were defined by the presence of asymmetric membrane thickening in multiple sections with or without a SB. Nerve terminals were followed through semi-serial sections to their originating dendrites below the IHC. They were further distinguished from efferent axons by the absence of vesicles. In mouse C57-29, semi-serial section analysis was conducted in 61, 59 and 54 terminals forming afferent synapses with IHCs at 8-, 16- and 32-kHz sites, respectively. Each afferent terminal contacted a single IHC.

Two morphologically distinct groups of terminals made contact with inner hair cells at three frequency locations in mouse C57-29. A group of nerve endings demonstrating conventional bouton-like morphology was designated simple terminals (Fig. 4A). A second group of larger nerve endings was designated as folded endings, and exhibited a novel morphologic feature consisting of an internalized double membrane that created an incomplete partition of the terminal (Fig. 4B). Although the double membrane and its intervening space appeared as a totally internalized organelle in some sections, evaluation of serial sections through the terminal revealed continuity of these membranes with the outer dendritic envelope as if it was invaginated (Figs. 5 and 6). The resulting membrane fold formed a septum that was oriented almost parallel to the IHC membrane, partially separating the terminal into inner and outer compartments (Figs. 4B and 6B). The inner compartment was post-synaptic to the IHC, whereas the outer compartment was separated from the IHC apposition and was sometimes post-synaptic to a vesiculated ending. These axodendritic synapses, which occurred exclusively at the outer compartment, were most commonly seen in the 8-kHz region (Fig. 5). Folded endings at 16 kHz were relatively flatter than those at the other frequency sites (Fig. 5B) and were not observed to receive axodendritic synapses from vesiculated axons, although such contacts were seen more proximally along the dendrite. The fold appeared to separate the population of mitochondria into an inner and outer aggregate. In some cases, the mitochondria were predominantly found in the inner compartment (Fig. 5), but in 62.1% of terminals, the volume density of mitochondria in the outer compartment exceeded that of the inner compartment. The propensity of mitochondria to aggregate in the outer compartment was greatest at 32 kHz ($t=2.42$, $p<0.05$) (Fig. 6A).

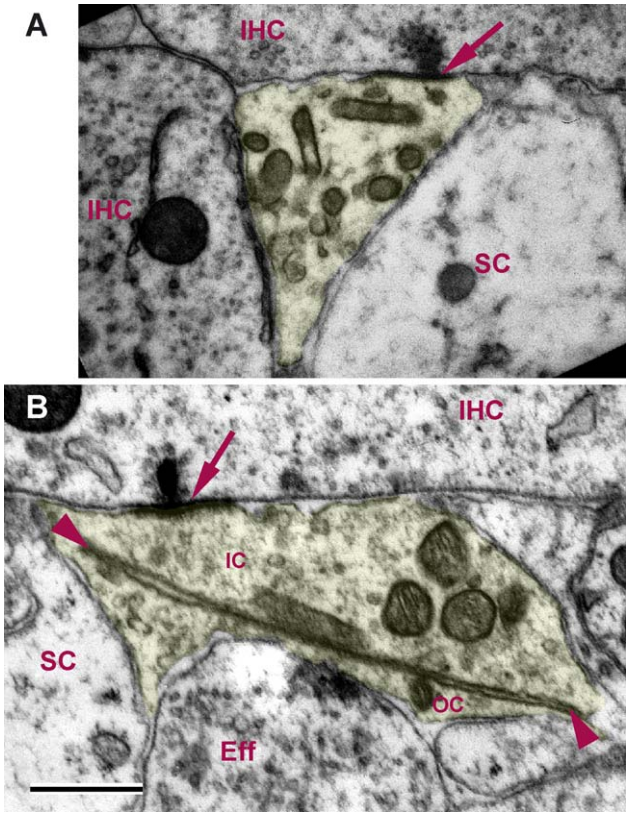

Fig. 4. Electron micrographs of two structurally distinct terminals forming afferent synapses (arrows) with IHCs. (A) Simple endings (colored yellow) are small and exhibit clear endosome-like vesicles, cytoplasm and mitochondria. (B) Folded endings (colored yellow) contain an internalized double membrane (arrowheads) that is continuous with the outer membrane, creating an incomplete partition of the bouton into an inner compartment (IC) that is adjacent to the cell apposition, and an outer compartment (OC) on the opposite side of the fold. Eff., efferent; SC, supporting cell. Scale bar 0.5 μm.

Simple endings formed afferent synapses that resembled those of folded endings (Fig. 7). Synapses formed by both ending types had a similar incidence of SBs (82% vs. 85%). In addition to the absence of an internalized double membrane, simple endings differed from folded endings in their terminal size, spatial distribution and the size and shape of their SBs.

Semi-serial section analysis of 10 IHCs from cochlea C57-29L revealed more folded endings (mean ± S.D.: 10.60 ± 3.27 per IHC) than simple endings (6.8 ± 3.94 per IHC; $t=2.35$, $p<0.05$; Fig. 8) in this animal. Folded endings were larger in volume (4.79 ± 2.22 μm^3, $t=8.38$, $p<0.0001$) and formed larger areas of apposition with IHCs (5.62 ± 3.25 μm^2, $t=6.48$, $p<0.0001$) as compared to simple endings (volume 2.16 ± 1.61 μm^3, apposition area 2.58 ± 2.6 μm^2) at all three frequency locations (Fig. 8). Folded and simple endings, however, did not significantly differ in their mitochondrial content as determined by the ratio of total mitochondrial to terminal volume (folded 0.13 ± 0.05, simple 0.13 ± 0.08) or the average number of mitochondrial profiles in each terminal profile (folded 4.41 ± 3.68, simple 4.15 ± 5.86). There was no difference in the area of electron dense membrane specialization formed by folded (0.27 ± 0.17 μm^2) and simple endings (0.23 ± 0.16 μm^2) at their synapses with IHCs. The maximum cross-sectional area of the SB was larger at synapses formed by simple (0.033 ± 0.036) compared to folded endings (0.025 ± 0.012), although the difference did not achieve statistical significance ($t=1.85$, $p=0.07$). There

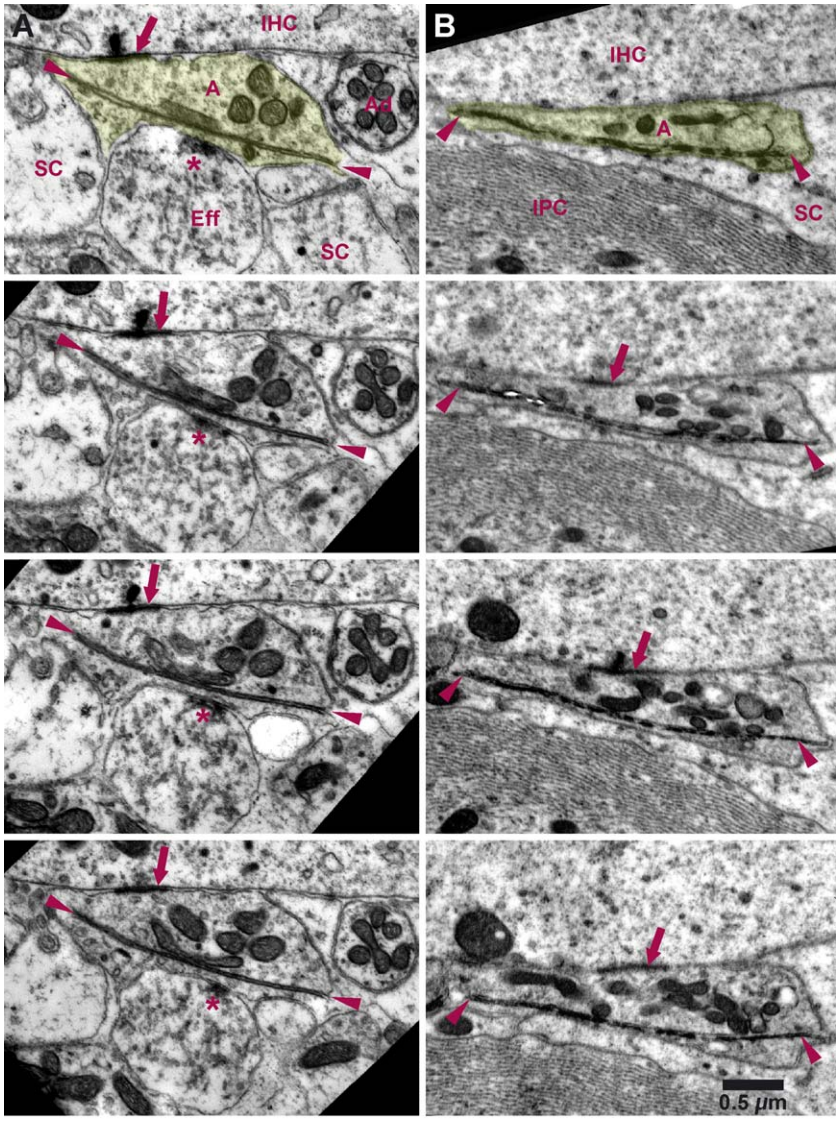

Fig. 5. Electron micrographs showing the internalized folds (arrowheads) in two representative folded endings (shaded yellow) forming afferent synapses (arrows) with IHCs in the 8- and 16-kHz regions. (A) Serial sections through an 8-kHz terminal with which an axodendritic synapse (asterisk) is formed at the outer compartment by a vesiculated fiber that is presumed to be an efferent (Eff). (B) Semi-serial sections (nos. 409, 413, 415 and 417) through a folded ending in the 16-kHz region where this ending type is flatter and less likely to receive axodendritic contacts. A, afferent; Eff., efferent; SC, supporting cell; IPC, inner pillar cell; Ad, afferent dendrite. Scale bar = 0.5 μm.

was a significant difference in the shape of SBs as measured by the ratio between the minimum and maximum cross-sectional dimensions, suggesting that the SBs associated with simple endings were relatively thinner (0.49 ± 0.14) than those of folded endings (0.55 ± 0.14, $t = 2.27$, $p < 0.05$).

Folded endings were observed in an additional 10 out of 11 C57BL/6J mice of various ages (Table 1) and were also found to be larger than simple endings in this sample. The folded morphology was consistent between animals as seen for three examples in Fig. 9. There were no discernible differences in terminal morphology between eight cochleae that were decalcified and four that were not. Profile area of terminals and the length of their apposition with IHCs were measured in six randomly sampled sections per IHC. This sampling protocol was applied to six IHCs from the C57-29L cochlea and was found to produce similar size distributions as those obtained when every other section was studied (Fig. 10). When 6 sections were sampled at approximately equal intervals through IHCs from 11 animals, the average profile area and apposition length of folded endings (1.10 ± 0.85 μm^2 and 1.74 ± 0.88 μm) were significantly larger than those of simple endings (0.78 ± 0.50 μm^2 and 1.29 ± 0.63 μm; $t = 4.77$, $p < 0.0001$ and $t = 5.47$, $p < 0.0001$).

The distribution of folded and simple endings around the side of the IHCs (Fig. 2B) was similar in mouse C57-29, but their distribution along the vertical axis of the cell was different. Simple endings were located on average closer to the inferior pole of the cell (3.36 ± 2.87μm; $t = 3.33$,

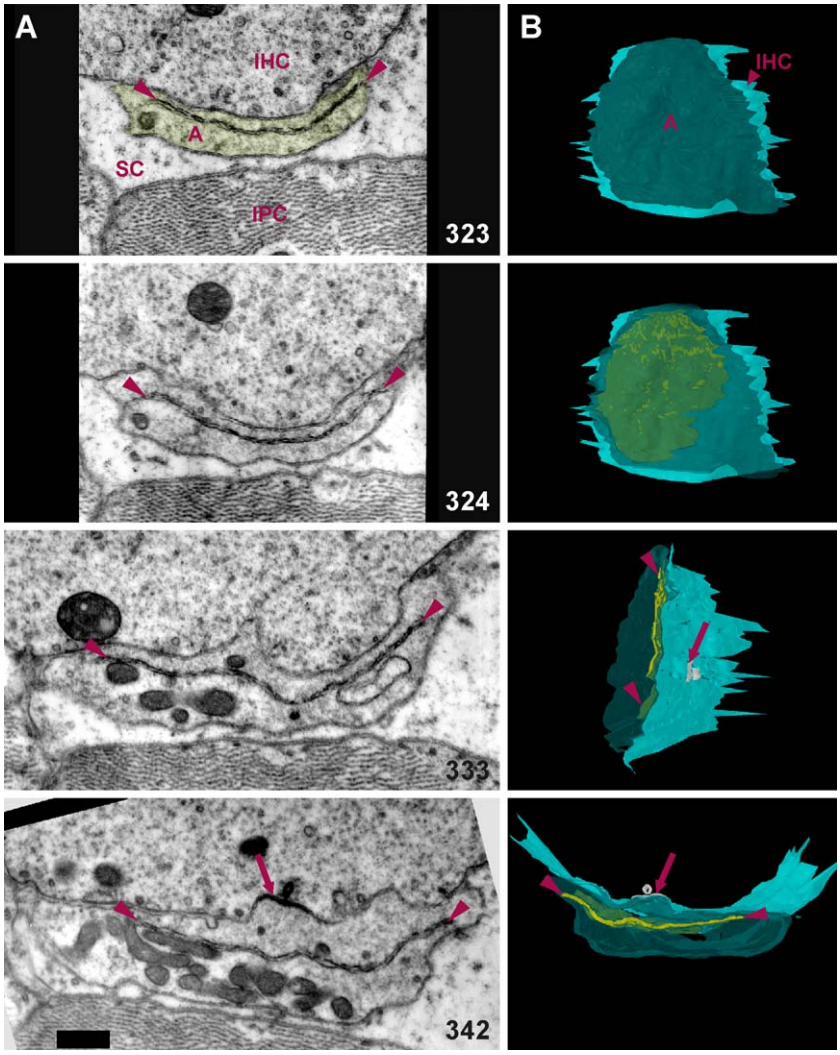

Fig. 6. Cross sectional (A) and three-dimensional anatomy (B) of folded terminal forming afferent synapse (arrow) with an IHC in the 32-kHz region. (A) Transmission electron micrographs of non-adjacent sections (nos. 323, 324, 333 and 342) through the folded terminal (shaded yellow) demonstrating a double membrane (arrowheads) that appears to be continuous with the outer membrane in the second section and is fully internalized in the third section. Note the preponderance of mitochondria in the outer compartment formed by the double membrane. Scale bar = 0.5 μm. (B) Four views of the three-dimensional reconstruction of the terminal presented in A. Panel 1 presents a surface view of the nerve ending (dark green) on the outer membrane of the IHC (aqua green). Panel 2 presents the same view but also reveals the space formed by the double membrane (yellow). Panels 3 and 4 demonstrate the almost parallel orientation of the double membrane envelop and the potential space that it encompasses, relative to the IHC apposition. A, afferent; SC, supporting cell; IPC, inner pillar cell.

$p < 0.005$) than were folded endings (4.84 ± 3.01 μm). Afferent synapses were typically located on the IHC facing the cochlear apex (109 apical, 42 basal). Although there was no difference in the volume of afferent terminals and their apposition areas at these locations, mitochondrial content was significantly higher in terminals on the pillar (volume fraction 0.15 ± 0.07; number per profile 6.07 ± 6.09) compared to the modiolar surface of IHCs (volume fraction 0.11 ± 0.05, $t = 3.57$, $p < 0.001$; number per profile 2.89 ± 1.9, $t = 3.72$, $p < 0.0005$). The volume fraction of mitochondria occupied by each terminal was estimated by taking the ratio of the sum of profile areas of mitochondria to that of nerve endings in semi-serial sections through two IHCs at 8, 16 and 32 kHz. A similar analysis performed in 6 sections randomly sampled from 12 animals (including 2 IHCs at the 16-kHz location in C57-29L) also revealed the presence of higher mitochondrial content in terminals on the pillar surface (0.18 ± 0.09) compared to the modiolar surface (0.15 ± 0.1, $t = 2.47$, $p < 0.05$).

4. Discussion

In this report, we describe the novel morphology of an afferent terminal in the cochlea. The outer membrane of some nerve terminals appears to be invaginated producing an internalized double membrane. This folded ending morphology was identified in the cochleae of 11 out of 12

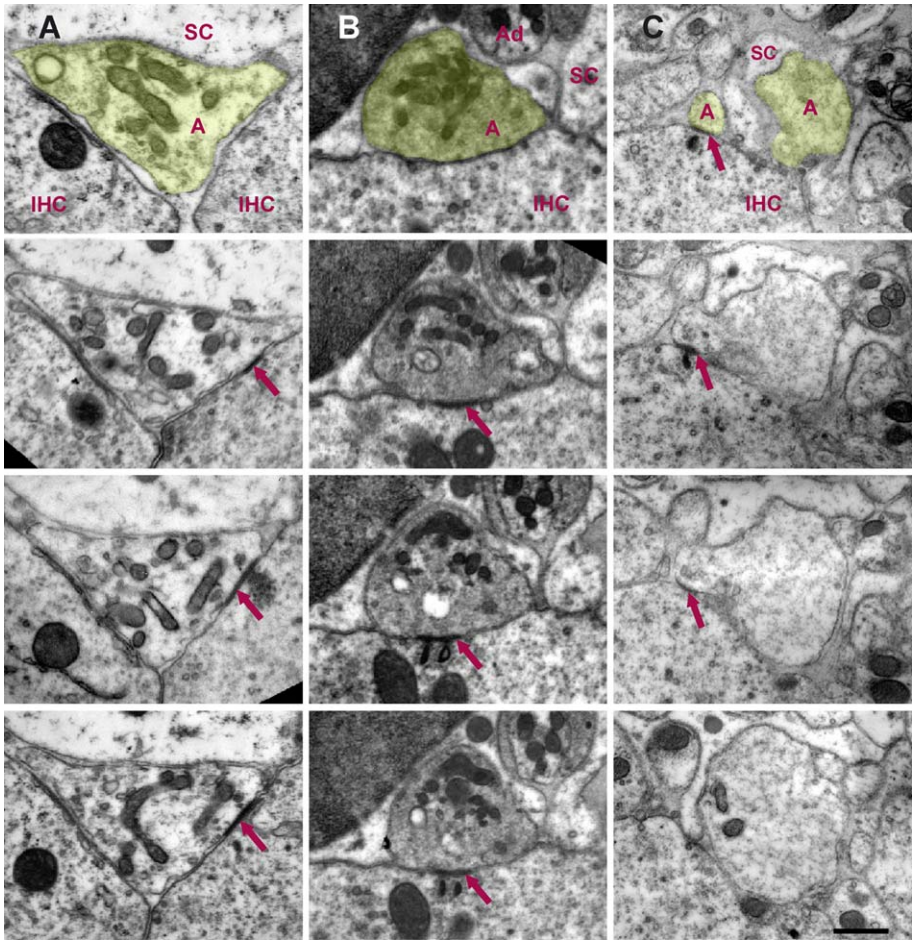

Fig. 7. Serial section electron micrographs through three bouton swellings (shaded yellow) that form afferent synapses (arrows) with IHCs in the (A) 8-kHz, (B) 16-kHz and (C) 32-kHz regions. Note the absence of an internalized double membrane. A, afferent; Ad, afferent dendrite; SC, supporting cell. Scale bar = 0.5 μm.

animals examined by transmission electron microscopy, all of which underwent in vivo intracochlear perfusion with a solution of 1% OsO_4 and 1% KFeCN. The internalized double membrane of folded endings persisted under various preparation conditions and is therefore unlikely to represent a histologic artifact. There was no disruption of the ultrastructural anatomy in adjacent simple terminals, efferent terminals, IHCs or supporting cells, and mitochondrial ultrastructure was well preserved within all cell types. Intact outer double membrane of mitochondria, parallel orientation of the cristae and dense matrix all indicate good quality tissue fixation [12]. The internalized double membrane forms a septum that partially divides the terminal into a post-synaptic and outer compartment. This septum could serve to isolate afferent and efferent synaptic activity or to compartmentalize metabolic activity of the terminal by aggregating mitochondria on either the outer or inner sides of the fold. The lower mitochondrial content of the inner compartment of terminals located in the 32-kHz region, for example, may be due to the loss of mitochondria in the post-synaptic cytoplasm due to glutamate induced excitotoxic injury [10,32]. Ultrastructural changes of this kind may represent early stages in disease progression of age-related and noise-induced hearing loss, and may correspond to early functional changes that are not explained by light microscopic findings [9].

Folded endings appear distinct from simple endings. Folded endings are larger in size and they form larger appositions with the IHC as compared to simple endings in both young and old animals. Folded endings tend to be closer to the nucleus, whereas simple endings tend to terminate closer to the base of the IHC. It could be argued that folded endings are simple endings undergoing pathologic changes or degeneration. If this were the case, however, a pathologic continuum that extends from normal simple endings through the folded ending stage to a terminal stage of degeneration should be evident. No such spectrum of terminal structure was seen on any of the IHCs. Dendrites that terminate as folded endings therefore appear to belong to a distinct group of afferent neurons that target more apical locations on the IHC compared to dendrites that form simple endings.

Differences in SB size and shape suggest that simple and folded endings have different physiologic attributes, and the

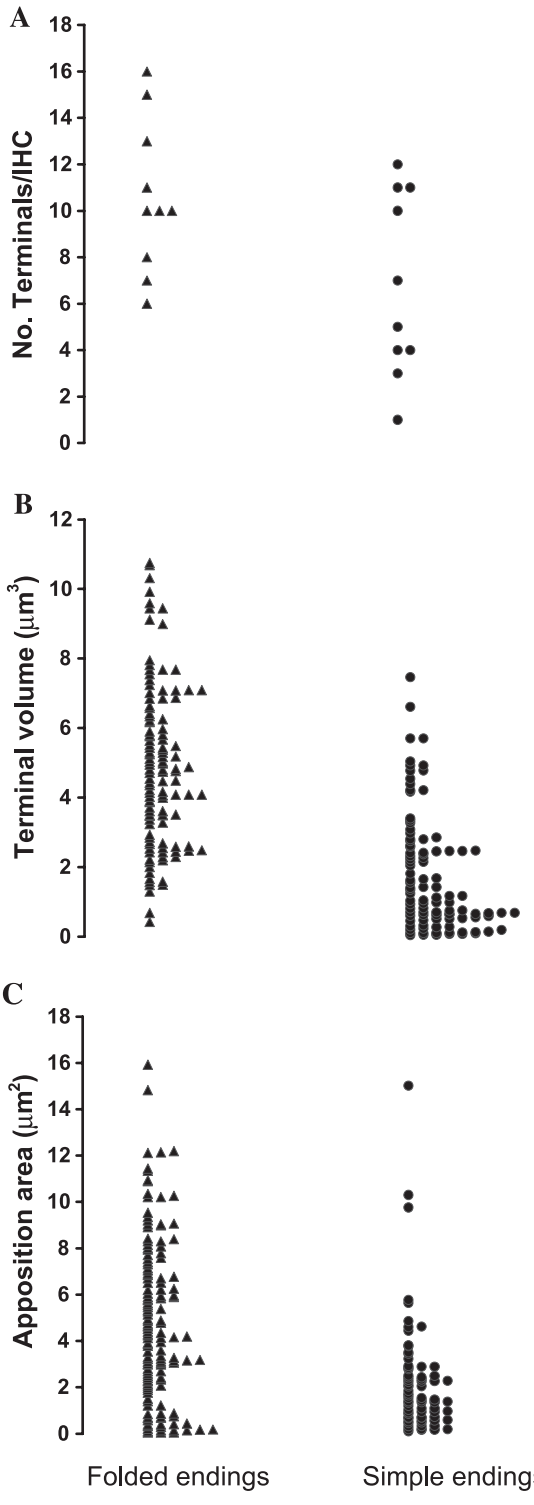

Fig. 8. Relative prevalence and size of folded versus simple endings innervating IHCs in the 8-, 16- and 32-kHz regions in a single C57BL/6J mouse cochlea (C57-29L). (A) There are generally more folded endings than simple endings innervating IHCs in this cochlea. Folded endings are larger in volume (B) and in their area of apposition with IHCs (C) as compared to simple endings.

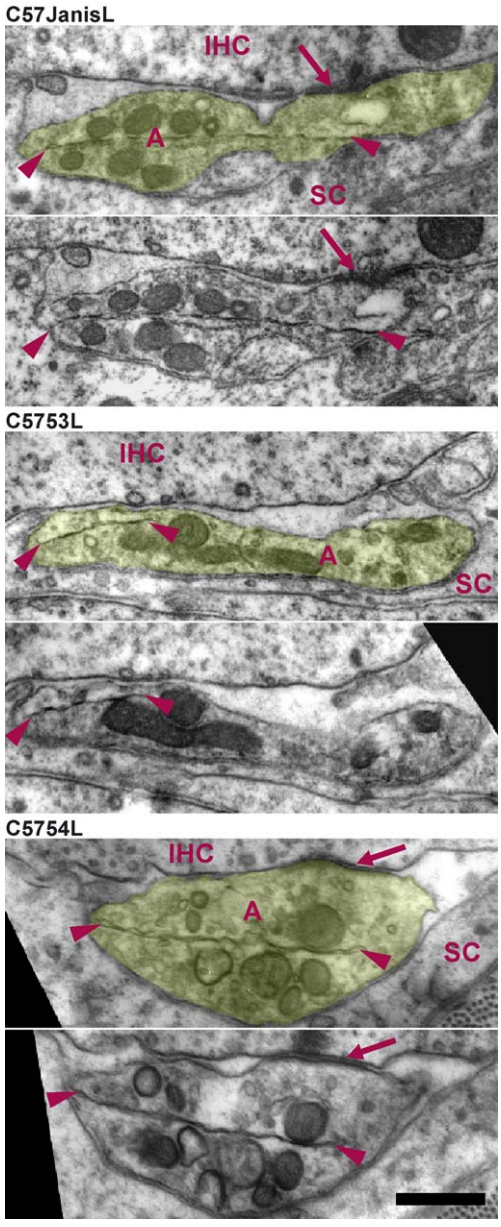

Fig. 9. Three pairs of adjacent sections showing examples of folded terminals (shaded yellow) found in the cochleae of other C57BL/6J mice. Arrowheads indicate internalized double membranes and arrows indicate afferent synapses. A, afferent; SC, supporting cell. Scale bar 0.5 μm.

correlation between mitochondrial content and spatial location suggests that afferents are also physiologically grouped according to other characteristics. The size and shape of SBs in cat, for instance, are correlated to spontaneous discharge rate, with more columnar-shaped and larger SBs having lower discharge rates [23]. Mitochondrial content was also correlated to spontaneous discharge rate in cat cochlea, but no difference was found between the mitochondrial content of simple and folded endings in C57BL/6J mice. As observed in cat [19], however, afferent terminals located on the pillar surface of the IHC contained a higher volume fraction and larger

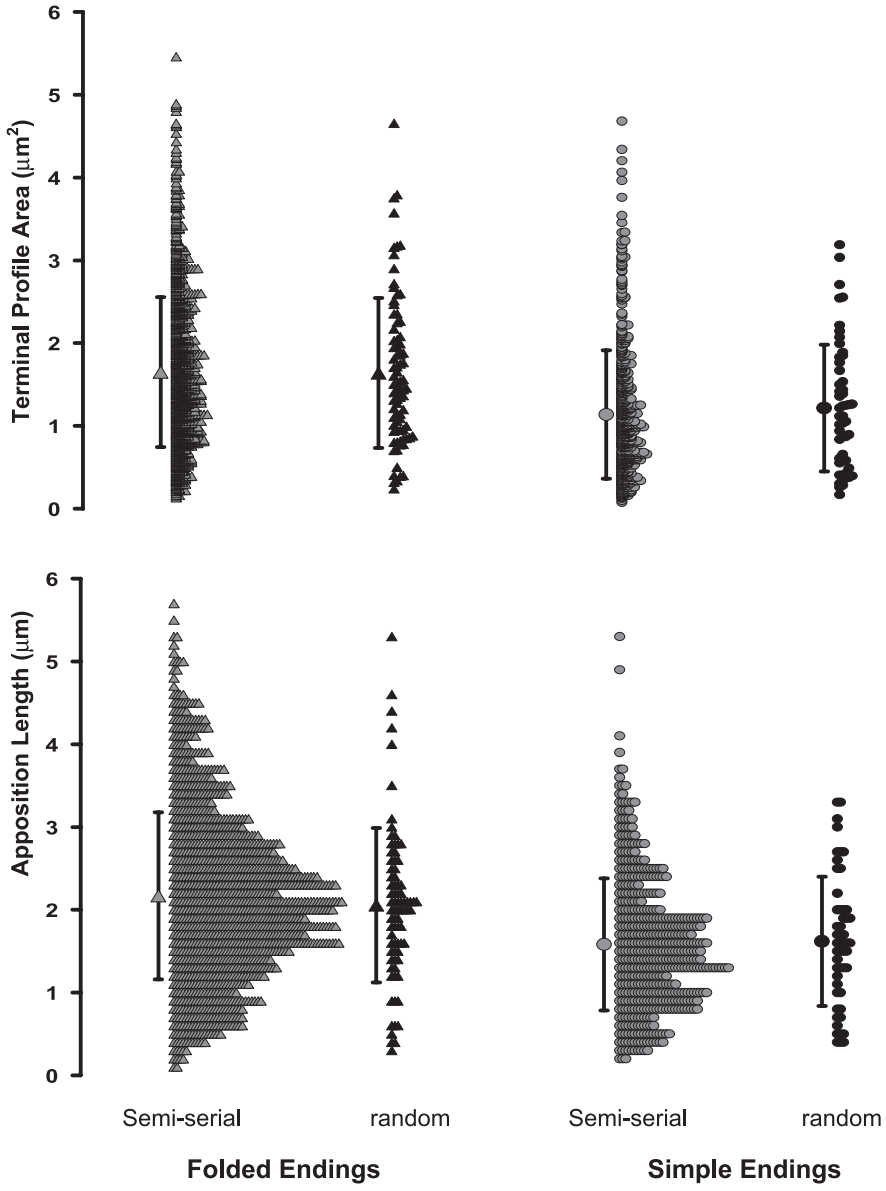

Fig. 10. Comparison of terminal size associated with six IHCs from mouse C57-29, using semi-serial sections (semi-serial) or six random sections per IHC (random). The distributions and means (error bars = S.D.) of profile area and apposition length were comparable for the semi-serial and sampled data, demonstrating larger folded compared to simple terminals using both protocols.

numbers of mitochondria per profile as compared to those on the modiolar surface. This consistent difference in mitochondrial content between terminals on pillar and modiolar surfaces, in both C57BL/6J mice and cats, suggests a biologically significant phenomenon that is independent of the fold morphology. The spontaneous and sound-evoked discharge characteristics of the auditory nerve are only now being investigated in mouse [45], and reveal many similarities to the cat [18], guinea pig [46] and gerbil [29]. Future correlations between terminal ultrastructure, auditory nerve response characteristics and the physiology of synaptic transmission from IHCs in the mouse [24] will contribute to our understanding of auditory transduction in the healthy and dysfunctional ear.

The absence of any description of folded swellings in the literature may reflect species and/or strain differences. Serial section analysis of IHC innervation in the cat, [19,22,43], gerbil [39] and guinea pig [11,38] report innervation densities that are comparable to those observed in the present study (Table 2), but membrane invagination or compartmentalization of terminals was not reported. Examination of axo-somatic and axo-dendritic contacts in the IHC region of neonatal and juvenile Harlan Sprague–Dawley ICR mice did not reveal folded swellings [40,41]. By comparison, the observation of en passant synapses between tunnel crossing afferents and IHCs in 12–17-day-old Harlan Sprague–Dawley ICR mice was not made in adult C57BL/6J mice in this study, suggesting that strain and age-differences may

Table 2
Comparative anatomy of IHC innervation

	Study	No. afferent terminals per IHC	No. synapses per terminal	% synapses without SB	Distinguishing characteristics of terminal subgroups
Mouse	Current study—adult C57BL/6J	10–20 (means 8 kHz—15.25, 16 kHz—19.67, 32 kHz—18.00)	1	16	Fold morphology, terminal size, vertical distribution, SB size and shape
Cat	Liberman et al. [19,20,22,23]	22–30	1	0	Spontaneous discharge rate, terminal size, mitochondrial content, pillar vs. modiolar location, SB size and shape, synapse morphology
	Spoendlin [42,43]	20	1		
Guinea pig	Hashimoto et al. [11]	25–27 (base), 15–17 (3rd turn)	1	19	Larger terminals on pillar side
Gerbil	Slepecky et al. [39]	15–20 apex (mean 18.75), 21–25 base (mean 22.25)	Not reported	Not reported	No consistent features found
Human	Nadol [26,27]	6–8	Up to 6. Means: basal turn 2.2, middle turn 1.3	17	Terminal size, smaller terminals on pillar side

SB, synaptic body.

be responsible for significant differences in afferent structure in mice. The random sampling of sections and the study of very young animals (birth to 50 days old) may be responsible for the failure to identify folded swellings in previous EM studies of C57BL/6J [37]. The folded morphology can also be misinterpreted if the outer compartment is mistaken for a supporting cell or another terminal forming an efferent contact. Serial section analysis is crucial for identification of the common origin of these compartments from the same axon.

The presence of folded endings in the ears of both 2-month-old C57BL/6J mice with normal hearing, and older animals with age-related hearing loss, suggests that this terminal morphology is neither pathologic nor related to the progressive hearing loss experienced by this mouse strain. A change in the prevalence of folded endings with age was not an objective of this study. These and other questions about the relationships between afferent terminal structure, age and hearing function are the subject of a stereological approach to study larger sample sizes [33]. This experimental approach is also needed to determine if the folded terminal morphology is generalized to murine strains. The apparent absence of these endings in juvenile Harlan Sprague–Dawley ICR mice [40,41] suggests that it is not.

A summary of our general findings is illustrated in Fig. 11 and a comparison to those in other species is made in Table 2. Although analysis of innervation density should be performed at comparable cochlear locations, the present data from a single mouse suggests that IHCs in C57BL/6J mice receive a similar number of afferents as do IHCs in guinea pig [11] and cat [20]. Furthermore, the innervation density in C57BL/6J mice (10–20 endings/IHC) is comparable to that estimated from fiber density and IHC counts in NMR1 mice (7–19 endings/IHC) [5]. Each ending tended to form a single synapse with the IHC, implying that each IHC gave rise to roughly 10–20 afferent synapses. Serial section analysis of two human IHCs revealed fewer afferent fibers per IHC but a similar number of afferent synapses per IHC because each fiber formed multiple synapses [26,27]. At present, it seems that IHC synaptic density is conserved across mammals. The study of a larger number of cells in human temporal bones at several known frequency locations is still needed for a comprehensive comparison of structural features of IHC innervation between human and C57BL/6J cochleae. Nevertheless, the C57BL/6J mouse remains an excellent animal model to study how the afferent sensory-neural interface in the organ of Corti responds to biological stressors.

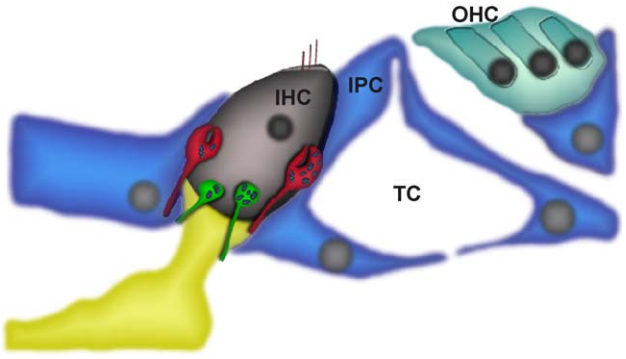

Fig. 11. This diagram summarizes the findings in this study. Folded endings (red) are larger and are spatially distributed closer to the nucleus compared to simple endings (green). Both ending types have similar mitochondrial content, but those located on the pillar surface adjacent to inner pillar cells (IPC) are more mitochondrion-rich than those located on the opposite (modiolar) surface. IHC, inner hair cell; IPC, inner pillar cell; OHC, outer hair cells; TC, tunnel of Corti.

Acknowledgements

This work was supported by NIH grants DC000143, DC00232 and DC05211, and grants from the American Hearing Research Foundation, Deafness Research Foundation and National Organization for Hearing Research. Thanks to the following individuals for their contributions to the work presented here: Sarah Francis, Karen Montey, Jenna Los, Sarah Lehar, Tan Pongstaporn and Yu Saito.

References

[1] C. Bertoni-Freddari, P. Fattoretti, Computer-assisted morphometry of synaptic plasticity during aging and dementia, Pathol. Res. Pract. 185 (1989) 799–802.
[2] C. Bertoni-Freddari, P. Fattoretti, R. Paoloni, U. Caselli, L. Galeazzi, W. Meier-Ruge, Synaptic structural dynamics and aging, Gerontology 42 (1996) 170–180.
[3] D.M.G. De Groot, Comparison of methods for estimation of the thickness of ultrathin tissue sections, J. Microsc. 151 (1988) 23–42.
[4] G. Ehret, Masked auditory thresholds, critical ratios and scales of the basilar membrane of the house mouse (*Mus musculus*), J. Comp. Physiol. 103 (1975) 329–341.
[5] G. Ehret, Quantitative analysis of nerve fibre densities in the cochlea of the house mouse (*Mus musculus*), J. Comp. Neurol. 183 (1979) 73–88.
[6] J.C. Falia, K.M. Harris, Cylindrical diameters method for calibrating section thickness in serial electron microscopy, J. Microsc. 202 (2001) 468–472.
[7] J.C. Falia, K.M. Harris, Extending unbiased stereology of brain ultrastructure to three-dimensional volumes, J. Am. Med. Inform. Assoc. 8 (2001) 1–16.
[8] E. Felder, A. Schrott-Fischer, Qualitative evaluation of myelinated nerve fibers and hair cells in cochleae of humans with age-related high-tone hearing loss, Hear. Res. 91 (1995) 19–32.
[9] H.W. Francis, D.K. Ryugo, M.J. Gorelikow, C.A. Prosen, B.J. May, The functional age of hearing loss in a mouse model of presbycusis: II. Neuroanatomical correlates, Hear. Res. 183 (2003) 29–36.
[10] H. Goulios, D. Robertson, Noise-induced cochlear damage assessed using electrophysiological and morphological criteria: an examination of the equal energy principle, Hear. Res. 11 (1983) 327–341.
[11] S. Hashimoto, R.S. Kimura, T. Takasaka, Computer-aided three-dimensional reconstruction of the inner hair cells and their nerve endings in the guinea pig cochlea, Acta Oto-laryngol. (Stockh.) 109 (1990) 228–234.
[12] M.A. Hayat, Principles and Techniques of Electron Microscopy, third edn., CRC Press, Boca Raton, 1989, 74–78 pp.
[13] K.R. Henry, R.A. Chole, Genotypic differences in behavioral, physiological and anatomical expressions of age-related hearing loss in the laboratory mouse, Audiology 19 (1980) 369–383.
[14] S. Hequembourg, M.C. Liberman, Spiral ligament pathology: a major aspect of age-related cochlear degeneration in C57BL/6 mice, JARO 2 (2001) 118–129.
[15] N.Y.-S. Kiang, T. Watanabe, E.C. Thomas, L.F. Clark, Discharge Patterns of Single Fibers in the Cat's Auditory Nerve, MIT Press, Cambridge, 1965.
[16] B.S. Krishna, A unified mechanism for spontaneous-rate and first-spike timing in the auditory nerve, J. Comput. Neurosci. 13 (2002) 71–91.
[17] H.-S. Li, M. Hultcrantz, E. Borg, Influence of age on noise-induced permanent threshold shifts in CBA/Ca and C57BL/6J mice, Audiology 32 (1993) 195–204.
[18] M.C. Liberman, Auditory-nerve response from cats raised in a low-noise chamber, J. Acoust. Soc. Am. 63 (1978) 442–455.
[19] M.C. Liberman, Morphological differences among radial afferent fibers in the cat cochlea: an electron-microscopic study of serial sections, Hear. Res. 3 (1980) 45–63.
[20] M.C. Liberman, Single-neuron labeling in the cat auditory nerve, Science 216 (1982) 1239–1241.
[21] M.C. Liberman, L.W. Dodds, Single-neuron labeling and chronic cochlear pathology: II. Stereocilia damage and alterations of spontaneous discharge rates, Hear. Res. 16 (1984) 43–53.
[22] M.C. Liberman, L.W. Dodds, S. Pierce, Afferent and efferent innervation of the cat cochlea: quantitative analysis with light and electron microscopy, J. Comp. Neurol. 301 (1990) 443–460.
[23] A. Merchan-Perez, M.C. Liberman, Ultrastructural differences among afferent synapses on cochlear hair cells: correlations with spontaneous discharge rate, J. Comp. Neurol. 371 (1996) 208–221.
[24] T. Moser, D. Beutner, Kinetics of exocytosis and endocytosis at the cochlear inner hair cell afferent synapse of the mouse, Proc. Natl. Acad. Sci. U. S. A. 97 (2000) 883–888.
[25] M. Mueller, K. von Huenerbein, S. Hoidis, J.W.T. Smolders, A physiological place-frequency map of the cochlea in the mouse, in: P.A. Santi (Ed.), 27th Mid-Winter Meeting of the Association for Research in Otolaryngology, Daytona Beach, FL, Abstract, vol. 423, 2004, p. 143.
[26] J.B. Nadol Jr., Serial section reconstruction of the neural poles of hair cells in the human organ of Corti: I. Inner hair cells, Laryngoscope 93 (1983) 599–614.
[27] J.B. Nadol Jr., Comparative anatomy of the cochlea and auditory nerve in mammals, Hear. Res. 34 (1988) 253–266.
[28] J.B. Nadol Jr., A.R. Thornton, Ultrastructural findings in a case of Meniere's disease, Ann. Otol. Rhinol. Laryngol. 96 (1987) 449–454.
[29] K.K. Ohlemiller, S.M. Echteler, Functional correlates of characteristic frequency in single cochlear nerve fibers of the Mongolian gerbil, J. Comp. Physiol. 167 (1990) 329–338.
[30] K.K. Ohlemiller, J.S. Wright, A.F. Heidbreder, Vulnerability to noise-induced hearing loss in 'middle-aged' and young mice: a dose-response approach in CBA, C57BL, and BALB inbred strains, Hear. Res. 149 (2000) 239–247.
[31] C.A. Prosen, D.J. Dore, B.J. May, The functional age of hearing loss in a mouse model of presbycusis: I. Behavioral assessments, Hear. Res. 183 (2003) 44–56.
[32] J.-L. Puel, J. Ruel, C. Gervais d'Aldain, R. Pujol, Excitotoxicity and repair of cochlear synapses after noise-trauma induced hearing loss, NeuroReport 9 (1998) 2109–2114.
[33] A. Rivas, P.R. Mouton, D.K. Ryugo, H.W. Francis, Stereological assessment of afferent innervation of inner hair cells in C57BL/6J mice, in: P.A. Santi (Ed.), 27th Mid-Winter Meeting of the Association for Research in Otolaryngology, Daytona Beach, FL, Abstract, vol. 424, 2004, p. 143.
[34] M.B. Sachs, Speech encoding in the auditory nerve, in: C.I. Berlin (Ed.), Hearing Sciences, Recent Advances, College-Hill Press, San Diego, 1984, pp. 263–307.
[35] R.A. Schmiedt, J.H. Mills, F.A. Boettcher, Age-related loss of activity of auditory-nerve fibers, J. Neurophysiol. 76 (1996) 2799–2803.
[36] H.F. Schuknecht, Auditory and cytocochlear correlates of inner ear disorders, Otolaryngol. Head Neck Surg. 110 (1994) 530–538.
[37] A. Shnerson, C. Devigne, R. Pujol, Age-related changes in the C57BL/6J mouse cochlea: II. Ultrastructural findings, Dev. Brain Res. 2 (1982) 77–88.
[38] J.H. Siegel, Serial reconstruction of inner hair cell afferent innervation using semithick sections, J. Electron. Micro. Tech. 15 (1990) 197–208.
[39] N.B. Slepecky, M.D. Galsky, H. Swartzentruber-Martin, J. Savage, Study of afferent nerve terminals and fibers in the gerbil cochlea: distribution by size, Hear. Res. 144 (2000) 124–134.
[40] H.M. Sobkowicz, S.M. Slapnick, L.M. Nitecka, B.K. August, Compound synapses within the GABAergic innervation of the auditory inner hair cells in the adolescent mouse, J. Comp. Neurol. 377 (1997) 423–442.

[41] H.M. Sobkowicz, S.M. Slapnick, L.M. Nitecka, B.K. August, Tunnel crossing fibers and their synaptic connections within the inner hair cell region in the organ of Corti in the maturing mouse, Anat. Embryol. 198 (1998) 353–370.
[42] H. Spoendlin, Innervation patterns in the organ of Corti of the cat, Acta Oto-laryngol. (Stockh) 67 (1969) 239–254.
[43] H. Spoendlin, The innervation of the cochlear receptor, in: A.R. Moller (Ed.), Basic Mechanisms in Hearing, Academic Press, New York, 1973, pp. 185–234.
[44] C.J. Sumner, E.A. Lopez-Poveda, L.P. O'Mard, R. Meddis, A revised model of the inner-hair cell and auditory-nerve complex, J. Acoust. Soc. Am. 111 (2002) 2178–2188.
[45] A.M. Taberner, M.C. Liberman, Response properties of simple auditory nerve fibers in CBA/CaJ mice, in: P.A. Santi (Ed.), 26th Mid-Winter Meeting of the Association for Research in Otolaryngology, Daytona Beach, FL, Abstract, vol. 176, 2003. p. 45.
[46] I.M. Winter, D. Robertson, G.K. Yates, Diversity of characteristic frequency rate-intensity functions in guinea pig auditory nerve fibres, Hear. Res. 45 (1990) 191–202.
[47] E.D. Young, M.B. Sachs, Representation of steady-state vowels in the temporal aspects of the discharge patterns of populations of auditory-nerve fibers, J. Acoust. Soc. Am. 66 (1979) 1381–1403.